PERGAMON

Journal of Atmospheric and Solar-Terrestrial Physics 63 (2001) 1199–1216

Journal of ATMOSPHERIC AND SOLAR-TERRESTRIAL PHYSICS

www.elsevier.nl/locate/jastp

Whistler-mode wave-injection experiments in the plasmasphere with a radio sounder

V.S. Sonwalkar[a,*], X. Chen[a], J. Harikumar[a], D.L. Carpenter[b], T.F. Bell[b]

[a] *Institute of Northern Engineering, University of Alaska Fairbanks, P.O. Box 755915, Fairbanks, AK 99775, USA*
[b] *Space, Telecommunications, and Radioscience Laboratory, Stanford University, Stanford, CA 94305, USA*

Received 21 February 2000; accepted 20 June 2000

Abstract

Whistler-mode wave-injection experiments with a high-altitude radio sounder offer an opportunity to greatly extend the observing power of satellites such as imager for magnetopause-to-aurora global exploration (IMAGE) when the satellite is within or near the plasmasphere or at low altitudes over the polar regions. We use as an example the radio plasma imager (RPI) instrument on IMAGE, which includes crossed 500-m electric antennas in the spin plane and a 20-m antenna along the spin axis (for reception only). The 500-m antennas approach a half-wavelength at whistler-mode frequencies in the 3–30 kHz range and should have a radiation efficiency of 1–10%. The wave power within ~100 km of the transmitter should be greater than that produced by wave injection from the ground-based very low-frequency (VLF) transmitter at Siple, Antarctica, thus making possible experiments on wave–particle energy and momentum exchange. We use ray tracings along a sample IMAGE orbit (polar, apogee $\sim 8R_E$) to show the conditions under which transmitted signals may return to the satellite as echoes, following reflection, or be observed by satellites of opportunity, such as EXOS-D. We find that ground reception of transmitted signals should be possible as a result of a linear mode conversion process in regions of ionospheric irregularities. We discuss the determination of wave-normal angles of returning signals, which will aid in identifying the signal path and obtaining information on plasma boundaries and irregularities. The science topics that may be addressed include: (1) investigation of the nonlinear process by which weak coherent waves excite VLF emissions; (2) probing plasmaspheric density structure, including plasmaspheric density cavities, field aligned waveducts, density irregularities in the plasmapause region, and the ionospheric density structure where conversion of whistler-mode wave energy to quasi-electrostatic lower hybrid (LHR) waves (and vice versa) can take place.

Keywords: Whistler-mode; Wave-injection; Plasmasphere

1. Introduction

Whistler-mode experiments with radio sounders offer an opportunity to greatly extend the observing power of satellites employing photon and radio techniques for purposes of "imaging" the Earth's magnetosphere. Such experiments, using for example, the radio plasma imager (RPI) on the imager for magnetopause-to-aurora global exploration (IMAGE) satellite, would complement the use of RPI as a high-altitude radio sounder in several ways: (1) their maximum potential would be realized when the spacecraft is within the plasmasphere and where sounding by RPI at frequencies above the *O* and *X* mode cutoff frequencies is limited to certain plasmaspheric regions Earthward of the spacecraft; (2) they would involve excitation by RPI of a "trapped" wave mode, as opposed to the free-space modes used in regular sounding operations; (3) they would involve important problem areas that are not confronted during regular free-space-mode sounding operations. Among these problems areas are: (1) the physics of wave–particle energy and momentum exchange within and near the plasmasphere; (2) the behavior of electric antennas at whistler-mode

* Corresponding author. Tel.: +1-907-474-7276; fax: +1-907-474-5135.
E-mail address: ffvss@uaf.edu (V.S. Sonwalkar).

1364-6826/01/$ - see front matter
PII: S1364-6826(00)00223-6

frequencies during in situ wave injection experiments; (3) the influence on whistler-mode propagation of density structure within and near the plasmasphere; (4) the downward penetration of the ionosphere by whistler-mode signals.

Whistler-mode wave injection from a satellite such as IMAGE, launched in March, 2000, can be a pioneering experiment. The operation of a whistler-mode transmitter in space has been a goal of space scientists for many years. Interest in such a project developed rapidly following the first successful ground-based whistler-mode wave injection experiments conducted in 1973 at Siple Station, Antarctica ($L = 4.2$) (Helliwell and Katsufrakis, 1974). It immediately became clear that relatively weak coherent signals injected into the outer plasmasphere could experience wave growth by 30 dB or more and be received at a conjugate ground station. The Siple experiments, in which the amplitude, phase, polarization, and frequency of the injected waves were controlled, substantially increased our understanding of the microphysics of wave–particle interactions (e.g. Helliwell, 1988; Gurnett and Inan, 1988). However, it was realized that these ground-based wave injection experiments had several inherent limitations: (1) relatively low-field strength of the injected waves ($B < 10$ pT), due to low antenna efficiencies ($< 2\%$) at VLF frequencies; (2) weak electromagnetic coupling of a ground-based source to the ionosphere and magnetosphere as a result of spreading of waves in the Earth–ionosphere waveguide, losses due to reflection and change of polarization at the Earth–ionosphere boundary, D-region absorption, and spreading of rays in the magnetosphere (e.g. Kintner et al., 1983); (3) limitation, to $\Delta L \sim \pm 0.5$, of the range of L-shells near the transmitter location that could be probed effectively (Carpenter and Miller, 1976; Carpenter and Bao, 1983); (4) restriction of injected wave-normal directions to angles near the vertical, due to the large refractive index in the ionosphere. It was recognized that a sufficiently powerful space-based VLF transmitter could overcome many of these limitations and provide a means to carry out a wide variety of active experiments not feasible from the ground (Inan et al., 1981). An important advantage of a ground transmitter is its ability to excite multiple ducts, whose ionospheric endpoints are distributed over some range of distances from the source.

In the late 1970s a NASA study group was formed to consider possible active wave experiments from the Shuttle (e.g. Inan et al., 1981). This group and its successor developed plans for a whistler-mode wave-injection mission called WISP, which was selected for a Shuttle flight in the mid 1980s. However, the project was cancelled after the Challenger accident in 1986. Scientists in the USSR and in countries formerly within USSR have also been seeking to implement wave-injection experiments. The low-altitude ACTIVNY satellite, launched in 1990, was designed to carry a VLF transmitter (nominal frequency $\sim$10 kHz, transmitter power $\sim$10 kW) coupled to a 20-m diameter loop antenna in a nearly polar orbit (83° inclination, apogee $\sim$2500 km, perigee $\sim$500 km). Conjunction experiments to detect ACTIVNY signals on the DE-1 and EXOS-D (Akebono) satellites as well as at several ground stations were carried out. However, no ACTIVNY signal was detected on satellites or at ground stations (Sonwalkar et al., 1994b). The lack of detectable signals was attributed to a failure of the antenna to deploy correctly. Thus, as the year 2000 approached, the long sought goal of a working VLF transmitter in space had yet to be realized.

The objectives of this paper are: (1) to introduce the concept of whistler-mode probing experiments by a sounder such as RPI on IMAGE, discussing issues related to feasibility; (2) to describe methods of determining the wave-normal direction of returned signals (echoes); (3) to briefly discuss a number of outstanding science problems that can be addressed with these experiments. Although our emphasis in the following is upon RPI on IMAGE, we intend much of the material to be relevant to the general problem of achieving whistler-mode wave injection in space.

2. Feasibility of whistler-mode experiments with RPI on image

The IMAGE satellite was launched on March 25, 2000 into an elliptical polar orbit with apogee at $\sim 8R_E$, perigee at $\sim$1000 km altitude and initial latitude of apogee 40°N. The RPI instrument consists of three orthogonal electric dipole antennas, two 500 m in length in the spin plane (contained in the orbital plane) and one 20 m in length along the spin axis. The long antennas are to be used for both transmission and reception and the short antenna for reception alone. The details of the RPI instrument are given by Reinisch et al. (2000). Most of the whistler-mode experiments on IMAGE will be performed when the satellite is within the plasmasphere or at low altitudes over the southern polar regions. Fig. 1 (adapted from notes by W. Calvert) shows two IMAGE orbits for the case of apogee at $\sim$40° north latitude; tick marks represent 1 h intervals. As apogee moves on a 1-year time scale between $\sim$40° and $\sim$90° north latitude, IMAGE may be estimated to spend between $\sim$30 min and 3 h within the plasmasphere on a given orbit, depending upon the L values of the plasmapause near the longitudes of plasmasphere penetration and egress. Those L values may vary from $\sim$2 to $\sim$8, depending upon disturbance levels, magnetic local time, and the still poorly known physics that govern plasmasphere erosion-recovery cycles (e.g. Carpenter and Lemaire, 1997).

The main issues related to the feasibility of whistler-mode experiments on the IMAGE satellite are: (1) antenna transmission and radiation characteristics at VLF frequencies; (2) wave-propagation paths and the possibility of wave reception on IMAGE (by the returning echo), on satellites of opportunity such as Akebono, and on the ground; (3) ability to measure the wave-normal direction of returning echoes; (4) potential of the injected waves to excite wave–particle interactions.

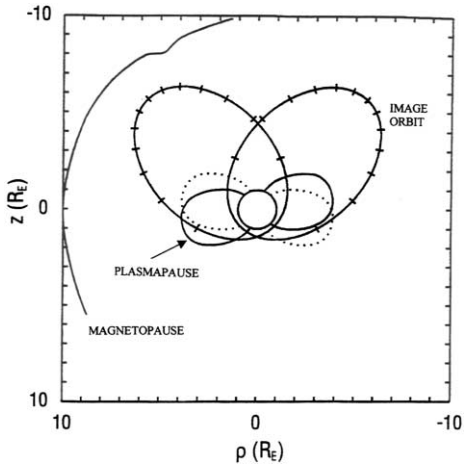

Fig. 1. Schematic showing two examples of IMAGE satellite orbits in relation to some of the principal magnetospheric boundaries and regions. Intervals between consecutive tick marks along the orbits correspond to time intervals of 1 h. A number of whistler-mode experiments may be conducted within the plasmasphere, where IMAGE spends from ~30 min to ~3 h during an orbit, depending on the latitude of apogee and plasmapause location.

2.1. Transmission of whistler-mode waves from the IMAGE satellite

The success of whistler-mode wave injection experiments from IMAGE will be limited by the amount and distribution of power that can be radiated into the magnetosphere from the antennas. Since whistler-mode frequencies are below the local plasma or gyrofrequency, whichever is lower, the properties of the RPI antennas should differ significantly from those prevailing at free-space-mode frequencies. The range of whistler-mode frequencies in the plasmasphere is from a few hundred Hz to a few tens of kHz, so that waves in the RPI transmitter frequency range 3–30 kHz can propagate in the whistler mode throughout much of the plasmasphere. At frequencies near half the local electron gyrofrequency the refractive index is around 20; propagation (group) velocities are low, of order $c/10$, so that pulse travel times over path segments several Earth radii in length are of order 1–2 s. A ~500-m antenna approaches a half wave length at VLF, and can have efficiencies of 1–10% when radiating in the whistler mode (see next section).

2.1.1. Antenna impedance and radiation efficiency at VLF

There is a need for study of electric antenna operations in the magnetospheric plasma when kV-level voltages are applied at whistler-mode frequencies. Under such conditions, the antenna response is expected to be a nonlinear function of the applied voltage, making it difficult to tune the antenna at a specific frequency. When voltage swings negative on one antenna element the sheath dimensions increase and the capacitance decreases. For voltage swinging positive, opposite changes occur. It is therefore important that measurements be made of the antenna voltage and current when RPI is operating at whistler-mode frequencies. Because of the high likelihood of strong wave excitation as well as the need to investigate unknowns associated with the antenna properties, RPI may be expected to serve as a testbed for future experiments targeted specifically at whistler-mode wave injection physics.

Previous works have obtained first-order estimates of electric dipole antenna impedance, efficiency, and radiation pattern using linear theory valid at low voltages (Mlodnosky and Garriott, 1963; Wang, 1970; Wang and Bell, 1972; Inan et al., 1981). Inan et al. (1981) have calculated the radiation efficiency of an electric dipole antenna as a function of frequency (3–30 kHz), electron density (10^4–10^7 el cm^{-3}), orientation with respect to the geomagnetic field (0–90°) and antenna length (200–1000 m). From this work, we estimate that the 500-m dipole antennas on IMAGE will have a whistler-mode radiation efficiency of 1–10% for frequencies in the 3–30 kHz range, with higher efficiency at the higher frequencies. Thus, we expect the long antennas to be capable of radiating approximately 0.1–1 W of whistler-mode power in the case of the anticipated 10 W of RPI transmitter power. The wave power within ~100 km of the transmitter should be greater than that produced by wave injection from the highly successful ground-based transmitter at Siple, Antarctica (e.g. Helliwell and Walworth, 1996).

2.1.2. Whistler-mode resonance cone and antenna radiation pattern

For whistler-mode frequencies above the local LHR (lower hybrid resonance) frequency, radiation from the RPI antennas will occur at wave-normal angles within a cone around the magnetic field direction called the resonance cone ($\theta_r \sim \cos^{-1}(f/f_{eH})$, where f_{eH} is the local electron gyrofrequency). The LHR frequency falls from ~10 kHz in the ionosphere to <1 kHz at several Earth radii. The resonance cone angle, at which the refractive index approaches infinity, varies between ~60° and ~75° for most of the expected choices of frequency for RPI. The shape of the refractive index surface inside the resonance cone is determined at a particular frequency by the variation in the magnitude of the refractive index μ as a function of the angle θ between the wave vector and the magnetic field. An important change in the shape of the surface occurs as frequency increases toward $f_{eH}/2$. The resonance cone angle becomes smaller and the surface becomes more bowl-like (e.g. Park, 1982).

Wang and Bell (1972) have determined the radiation patterns of arbitrarily oriented point electric and magnetic dipoles in a cold multicomponent magnetoplasma. They find that focusing effects in the radiation patterns due to the geometrical properties of the refractive index surface

tend to dominate the radiation distribution over the entire range $4.6 f_{pH} \leqslant f \leqslant f_{eH}$, where f_{pH} is the proton gyrofrequency. Focusing effects are particularly strong in the range $f_{LHR} \leqslant f \leqslant f_{eH}/2$, where the major lobe of the radiation pattern lies along the static magnetic field (30–50 dB radiation gain) and the lobe intensity varies inversely as the first power of the distance between source and observer rather than as the square of that distance. The gain in the direction of the static magnetic field is maximized when $f = f_{eH}/2$. For frequencies in the range $f_{eH}/2 < f \leqslant f_{eH}$, up to ~30–40 dB gain is obtained in a direction oblique to the geomagnetic field. The antenna radiation patterns described by Wang and Bell (1972) are for a point dipole, and we may expect additional structure in the pattern for a dipole of finite length.

Focusing of radiation can also occur for waves with wave-normal angles close to the Gendrin angle ($\theta_G \sim \cos^{-1}(f/2f_{eH})$ since their ray directions will be bunched around the direction of the geomagnetic field (Helliwell, 1995). Thus it seems clear that focusing effects should be important in the radiation.

2.2. Signal propagation paths

In this section, we discuss the possibility of reception of transmitted signals by (1) the IMAGE satellite, (2) a satellite of opportunity, such as Akebono, and (3) ground VLF stations. To determine the accessibility of RPI signals to IMAGE itself and to Akebono we have performed ray tracing simulations in a model magnetosphere. We have used the Stanford 2-D ray-tracing program which employs a dipole field model, a diffusive equilibrium model for density along field lines within the plasmasphere, and an (R^{-n}) density falloff outside the plasmasphere (Inan and Bell, 1977). In our calculations we assume the plasmapause to be at $L = 4$ and an $R^{-4.5}$ density variation outside the plasmasphere so as to closely match a "collisionless" model (R^{-4}) at middle invariant latitudes (e.g. Eviatar et al., 1964; Angerami and Thomas, 1964; Angerami, 1966) as well as an R^{-5} empirical model at high latitudes (e.g. Persoon, 1988).

2.2.1. Possibility of reception of returning echoes on IMAGE

Most whistler-mode wave activity in the magnetosphere involves the so-called "nonducted" propagation, in which the wave-normal angles are not constrained to remain within a narrow range around the geomagnetic field direction as the wave propagates. In general, all wave-normals inside the resonance cone will be excited during an RPI transmission, with focusing in certain directions as noted above. For most of the excited wave-normals, the associated ray paths are not expected to lead back to the satellite. This is because of ray-path bending attributable to the large-scale inhomogeneities in the magnetic field and plasma. However, for certain injected wave normals, the radiated energy propagating along nonducted raypaths may be expected to return to IMAGE following reflection at distant locations.

Two types of reflection mechanisms are possible for whistler-mode waves propagating in the magnetosphere: (1) magnetospheric reflection (MR), and (2) ionospheric reflection. In MR, the wave is reflected at an altitude (generally lower than that of the satellite) where the transmitted frequency and the LHR frequency become equal. At this location the local refractive index surface changes from an open conical shape ($f > f_{LHR}$) to a closed surface ($f < f_{LHR}$), and reflection occurs as the ray direction is flipped by 180° (Kimura, 1966). In the case of an echo returning to its in situ source, this process has been called by Edgar (1972) the "boomerang mode". Ionospheric reflection occurs at the Earth–ionosphere boundary and is a result of large differences between the refractive index (μ) values on opposite sides of the boundary, μ being ~10–20 on the ionosphere side and unity on the Earth side. For a ray to return to the satellite by ionospheric reflection it is necessary that it retrace its path, which requires that it be incident on the Earth–ionosphere boundary with its wave normal aligned along the local vertical (assuming a horizontally stratified ionosphere). Fig. 2 shows examples of rays launched at points along an IMAGE orbit when the latitude of apogee is ~40°N. Wave frequency (f), initial wave-normal angle (θ) and the round trip group delay (t_g) are indicated. Note that a wave-normal angle of 0° is directed along the magnetic field towards the southern hemisphere. Positive angles are directed towards the lower L-shells, negative angles toward the higher L-shells. In Fig. 2a, a ray at 3 kHz launched at ~$5R_E$ geocentric distance at high northern polar latitudes returns to the satellite after an ionospheric reflection, while in Fig. 2b a ray at 3 kHz launched just outside the plasmapause near the equator returns after a magnetospheric reflection. In both figures, an example is shown of a reflected 3 kHz ray that does not return to the satellite.

A return echo is also possible when the injected waves are guided by density gradients, as in a field-aligned density enhancement (ducted propagation) or by the density gradient at the plasmapause. Fig. 2c shows a case in which a 10-kHz ray launched just outside $L = 4$ returns to the satellite after being guided by the plasmapause gradients and ionospherically reflected at the Earth–ionosphere boundary. Fig. 2d shows the case of a 10-kHz ray launched at the equator within a duct centered at $L = 3$ and ionospherically reflected back to the satellite. For waves to be trapped in a duct it is necessary that the satellite be either inside a duct or nearby, within a few hundred km, and that $f < f_H/2$, where f_H is the gyrofrequency at the satellite location (Smith and Angerami, 1968). The probability of this type of propagation on a given orbit is limited, since ducts are believed to occupy only a small fraction of the magnetospheric volume at a given time (Burgess and Inan, 1993; Sonwalkar, 1995). However, ducted whistlers propagating in the plasmasphere have been observed at a ground station in Antarctica over

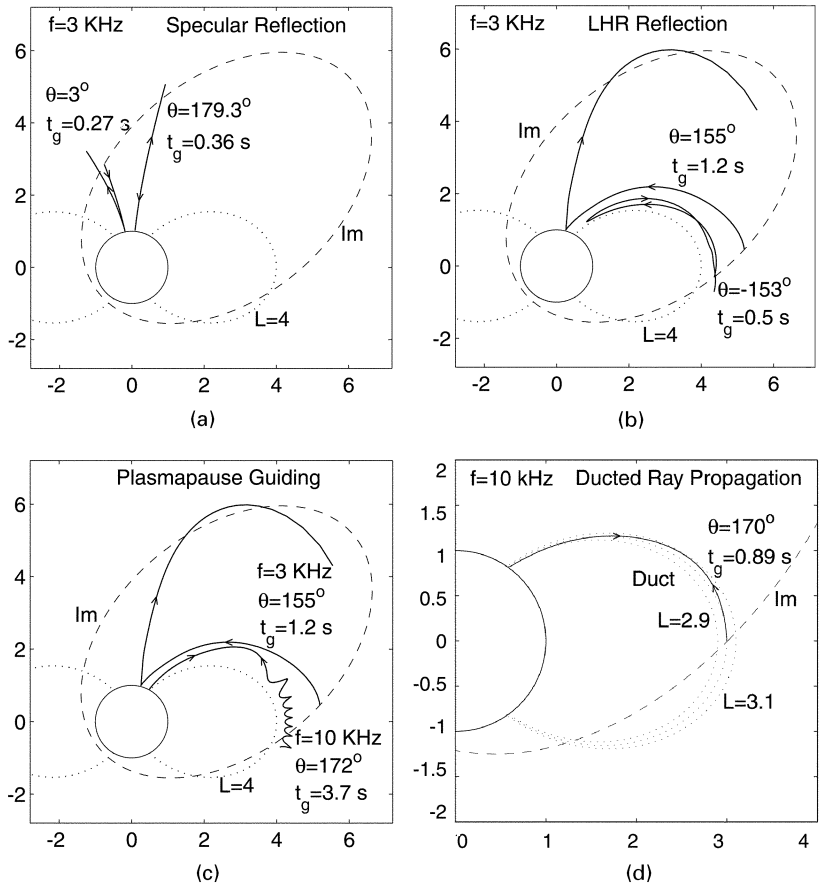

Fig. 2. RPI signals can return (as echoes) to the IMAGE satellite along four distinct types of propagation paths. (a) Injected RPI signals propagate in a nonducted mode and are ionospherically reflected at the lower boundary of the ionosphere. Two rays are shown, one that returns and one that does not return. Wave frequency (f), initial wave-normal angle (θ) and the round trip group delay (t_g) are indicated on the figure. (b) RPI signals return to the satellite after a magnetospheric reflection at an altitude where $f = f_{LHR}$. This mode of reflection is possible only for frequencies below the maximum lower hybrid resonance frequency in the topside ionosphere. (c) RPI signals return to IMAGE after being guided by the plasmapause. (d) RPI signals return to IMAGE after propagating in field-aligned ducts (ducted propagation) and reflecting at the bottom of the ionosphere.

most the 24 h and under a wide range of geomagnetic conditions (e.g. Carpenter, 1966), so the probability of duct excitation by IMAGE on one or more orbits per month must be considered high.

Figs. 3a–e are the result of ray tracings to see over which segments of the IMAGE orbit in Fig. 2 returning echoes at particular frequencies from 3 to 30 kHz should be possible as the result of ionospheric or LHR reflection. Rays were continuously injected along the IMAGE orbit in order to determine those segments of the orbit where returning echoes can be received. As an illustration, a few examples of returning ray paths are shown in Figs. 3a–e. Fig. 3a shows (1) the contiguous orbit segment beginning at A and extending to E over which return echoes are possible after an ionospheric reflection, and (2) the orbit segments from B to C and from D to F over which return echoes are possible after LHR reflection. A similar pattern is found for 5 kHz (Fig. 3b), but as frequency increases to 10–30 kHz (Figs. 3c–e), only ionospheric reflection is possible and the orbital segments involved become more restricted in altitude. This frequency dependence arises in part because the highest f_{LHR} in the magnetosphere is typically $\sim$10 kHz, so that most frequencies $f > 10$ kHz can only undergo the ionospheric type of reflection.

It is not yet possible to predict the intensity of the various echoes returning to the satellite. In the illustration of Fig. 2, only a narrow range of wave normals around the one indicated may be expected to contribute to the returning echo. Losses of the order of 10–15 dB during nonducted propagation arise due to the spreading of ray paths. In the case of ionospheric reflection, additional losses occur due to collisional absorption in the lower ionosphere. Depending on

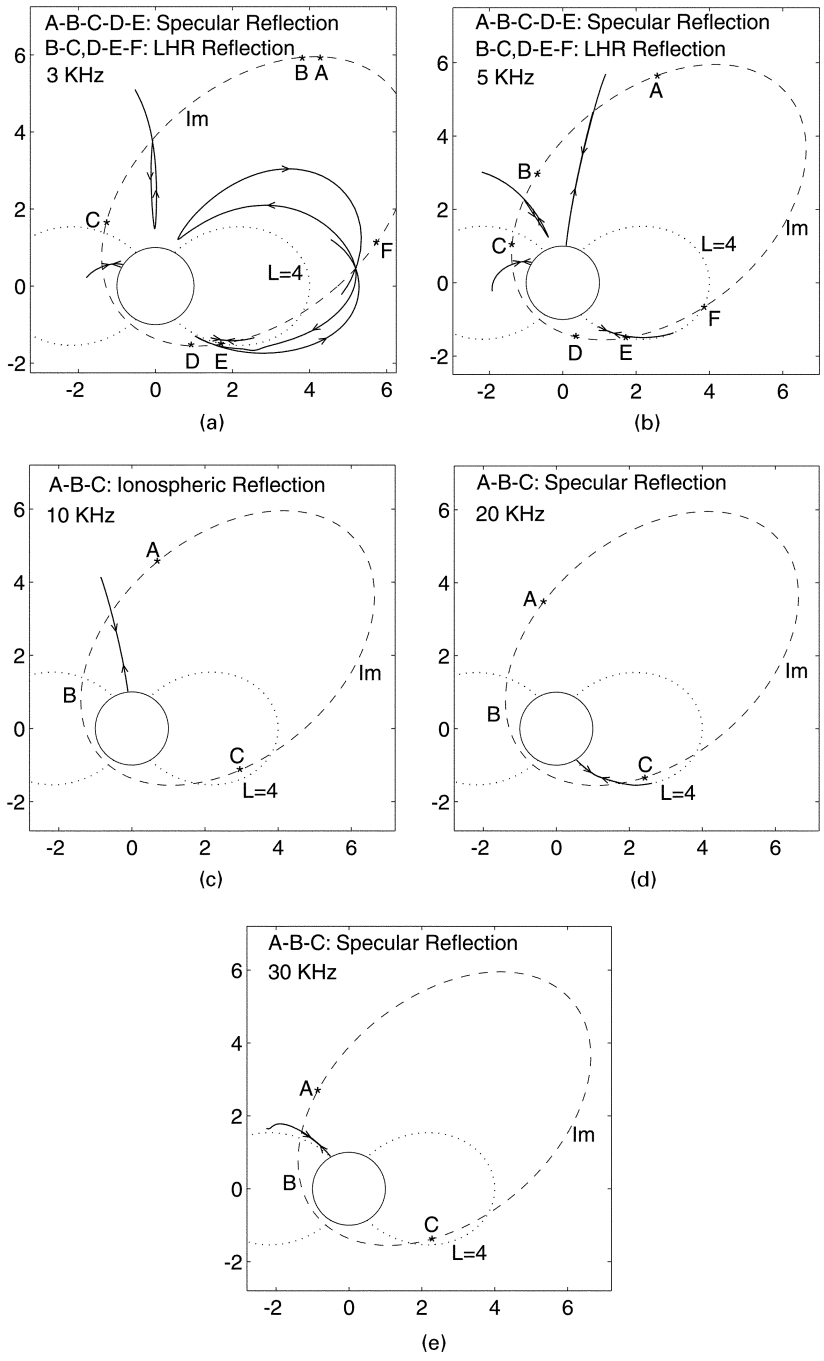

Fig. 3. Portions of a sample orbit along which RPI echoes at a particular frequency can return to IMAGE (Im). (a) Contiguous orbit segment A–B–C–D–E depicts the region of accessibility of 3 kHz signals after ionospheric reflection. Orbit segments B–C and D–E–F depicts the region of accessibility of 3 kHz signals after magnetospheric reflection (LHR reflection). (b)–(e) similar information for 5, 10, 20, and 30 kHz. At higher frequencies ($f > f_{\mathrm{LHRmax}}$), only ionospheric reflections are possible (see text for details).

frequency and wave-normal direction, these losses are of the order of 10–40 dB in the daytime and 2–4 dB at nighttime (Helliwell, 1965). The losses increase roughly as the square root of the frequency and as $\cos\theta^{-3/2}$, where θ is the wave-normal angle in the ionosphere. In the case of ionospheric reflection, the intensity of the returning echo will thus depend on the radiated power, which increases with frequency, on ionospheric absorption, which also increases

with frequency, and on spreading losses. The magnitude of the reflection coefficient will be close to 1, even if, because of the vertical wave normal angle, a small fraction of the wave energy is transmitted across the boundary. Horizontal density gradients at the ionospheric reflection altitude may also play a role in determining the intensity of a returning echo after an ionospheric reflection. It should be noted that in the outer plasmasphere ($L \cong 2$–4), the energetic electron particle distribution is generally amplifying for whistler-mode waves that are near the magnetic equator and have wave normals within $\sim 45^\circ$ of the geomagnetic field direction (Bell et al., 2000). Following particle injection events, gains of 20–30 dB appear common. Also, as noted above, there is the possibility of 30–50 dB radiation gain in the static magnetic field direction for RPI frequencies near $f_{eH}/2$.

Figs. 2 and 3 show a wide range of possible ray paths both inside and outside the plasmasphere. As apogee latitude increases with time towards 90°, we expect the regions of accessible return echoes to change, but the general conclusions drawn above should remain the same.

2.2.2. Signal reception on the Akebono satellite

There is a good chance that RPI signals will be detectable on the Akebono satellite (apogee ~9000 km, perigee ~270 km, inclination =75°) (Tsuruda and Oya, 1993). Previous work (Sonwalkar et al., 1994b) with 3-D ray tracings in the magnetosphere has shown that rays injected in the magnetic meridional plane can spread about 5–10° in longitude and that those injected in the plane perpendicular to the meridional plane spread about 30° in longitude. Thus, conjunction experiments between Akebono and IMAGE should be planned when the two satellites are within ~30° in longitude. The rays injected from IMAGE can reach Akebono via nonducted ray paths directly or after magnetospheric reflection, as shown in Fig. 4. With relatively small losses in the magnetosphere, we would expect RPI signals to be received on Akebono during most conjunctions. The Akebono satellite plasma wave receiver is equipped with three electric and three magnetic antennas, and is capable of making wave-normal measurements (e.g. Sawada et al., 1993).

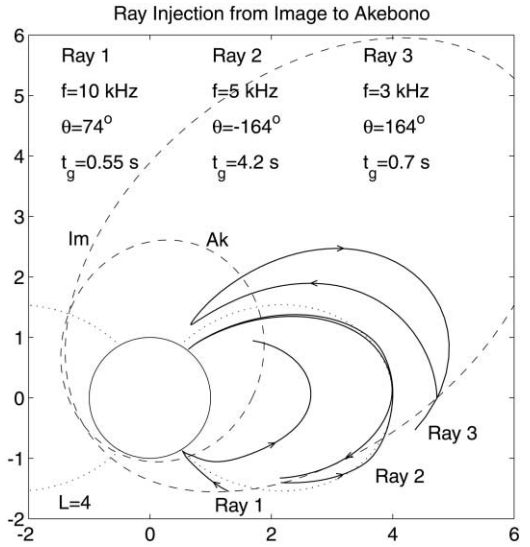

Fig. 4. Sample ray paths illustrating possible RPI signal reception on the EXOS-D satellite, called Akebono (Ak) (apogee ~9000 km, inclination 75°). RPI signals can reach Ak: (1) along an initially Earthward-directed nonducted path, either before or after ionospheric reflection at the ionosphere boundary (ray 1); (2) along an initially outward directed nonducted path, before and/or after ionospheric reflection at the ionosphere boundary (ray 2); (3) along a nonducted path, before or after magnetospheric reflection. In some cases, as in that of ray 3, RPI signals may be detectable on both the IMAGE and Akebono satellites. In general, the IMAGE and Akebono satellites need to be within 15° magnetic longitude for RPI signals to be detectable on Akebono (Sonwalkar et al., 1994b).

2.2.3. Signal reception on the ground: possibility of ionospheric penetration

In principle, part of each whistler-mode transmission from RPI should penetrate the ionosphere and be incident upon the antennas of ground receivers. This can be argued in terms of reciprocity and the expectation that transmissions from the ground can illuminate large portions of the plasmasphere (e.g. Sonwalkar and Inan, 1986). As in the case of the boomerang mode discussed above, only a particular initial wave-normal or range of wave-normals would be involved, such that when the ray reaches ionospheric heights the wave vector is close enough to the vertical to avoid internal reflection (Helliwell, 1965). Typical values of the "transmission cone" half-angle are ~3–5° for mid-to-high latitudes. It was noted above that an RPI signal may return to IMAGE by ionospheric reflection when the signal is normally incident on the Earth–ionosphere boundary. Therefore, we expect RPI signals to be capable of reaching the ground over those IMAGE orbit segments in Fig. 3 along which echoes returning to IMAGE are possible. Whether such signals can actually be detected at a ground station over and above the local noise will depend upon factors such as the power injected at the required wave normal angle, spreading losses of the order of 10–20 dB, D-region absorption loss (discussed above), and losses in the Earth–ionosphere waveguide, of the order of ~7 dB per 100 km (Tsuruda et al., 1982). It is interesting to note that a ground transmitter signal, seen on a satellite, enters the ionosphere with a nearly vertical wave-normal angle. Thus the path taken by a ground transmitter signal seen on the satellite is roughly the same as that taken by a signal from the satellite to the ground. RPI on IMAGE thus provides an opportunity to study such reciprocal propagation of VLF signals.

Most of the wave energy from RPI will not fall within the required cone of angles around the vertical, and some redirection of the waves will therefore be required, either

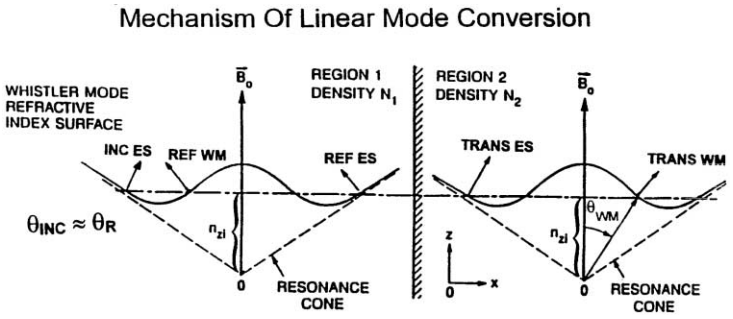

Fig. 5. Geometrical description of linear mode conversion of whistler-mode waves by scattering of a large wave-normal-angle wave into small wave-normal-angle waves at the boundaries of meter-scale irregularities. An incident large wave-normal-angle ($\theta \sim \theta_r$) whistler mode wave (INC ES) is converted to a low wave-normal-angle whistler-mode transmitted wave (TRANS WM), a reflected wave (REF WM), a quasi-electrostatic reflected wave with large wave-normal angle (REF WS), and a transmitted electrostatic wave (TRANS ES). Snell's law requires that the parallel refractive index (n_z) for all the waves must be the same as that of the incident wave (n_{zi}) (adapted from Bell and Ngo, 1988).

by a scattering process during encounters with meter-scale irregularities (described below) or by ray bending in larger scale density structures (James, 1972; Sonwalkar et al., 1984).

Current work on the problem of ionospheric penetration by auroral hiss (Sonwalkar and Harikumar, 2000) indicates that the meter-scale (1–100 m) irregularities present at altitudes below 5000 km can scatter a small fraction (0.1–10%) of incident large-wave-normal-angle whistler-mode waves into small-wave-normal-angle waves, which can then propagate to the ground without being totally internally reflected. In the presence of such meter scale irregularities, downcoming nonducted waves have the potential to penetrate the ionosphere and be detected at ground points, provided that the amplitude of the incident waves is high enough to overcome the additional propagation losses to be expected. Auroral hiss is regularly observed on the ground but is originally very strong. Thus, for RPI signals to achieve penetration, it becomes important to estimate the amount of power that will be needed.

One mechanism by which the wave-normal angles of VLF waves can be modified is the passive linear scattering mechanism described by Bell and Ngo (1988, 1990) and outlined in Fig. 5. In this mechanism, as a consequence of matching boundary conditions in a cold magnetoplasma, a large wave-normal-angle wave incident on a plasma irregularity (INCES) excites whistler-mode waves with small and large wave-normal angles on both sides of the irregularity (two reflected and two transmitted waves). The wave-normal matching condition requires that the component of the wave refractive index parallel to the boundary of the irregularity be the same for all excited waves and be equal to that of the incident wave.

The boundary conditions allow us to determine the amplitudes of the excited, reflected, and transmitted small- and large-wave-normal waves. Using a computer program originally developed by Ngo (1989) and modified by one of us (JH), we have calculated the fraction of the incident power in a large-wave-normal-angle whistler-mode wave that is converted into waves with wave-normal angle small enough to fall within the ionospheric transmission cone. Fig. 6 shows the results of computation carried out at 2000 km altitude for invariant latitudes of 50° (within the plasmasphere) and 70° (auroral zone), respectively. A Gaussian density distribution was assumed for the irregularity. The local electron densities are 1350 and 1220 el cm^{-3} for the plasmaspheric and auroral zones, respectively. The wave-normal direction of the downcoming whistler-mode wave was adjusted so that the transmitted small-wave-normal whistler-mode wave (TRANS WM in Fig. 5) was within about ~5° of the vertical, a typical value for the transmission cone half angle. The incident downcoming wave-normal required for this was within 1° of the local resonance-cone angle. Fig. 6 shows the ratio of transmitted to incident power for 10 kHz (top two panels) and 30 kHz (bottom two panels) as a function of irregularity amplitude ($\Delta N_e/N_e$) for various sizes of irregularities in terms of wavelength. In the plasmaspheric zone values of λ are ~0.86 and ~1.95 m for $f =$ 30 and 10 kHz, respectively. In the auroral zone corresponding values of λ are ~0.85 and ~2.9 m. Fig. 6 shows that at 10 kHz about 1–5% of the power in the incident large-wave-normal-angle whistler-mode wave is converted into that of a small-wave-normal-angle whistler-mode wave that can penetrate to the ground. The amount of power converted to low-wave-normal-angle waves at 30 kHz is much smaller, less than 0.1%.

Other mechanisms to convert small-θ whistler-mode waves to large-θ whistler mode waves have been proposed by Titova et al. (1984) and Groves et al. (1988). Groves et al. (1988) have suggested a nonlinear mechanism by which ionospheric density fluctuations with scale lengths of several tens of meters scatter VLF waves to produce

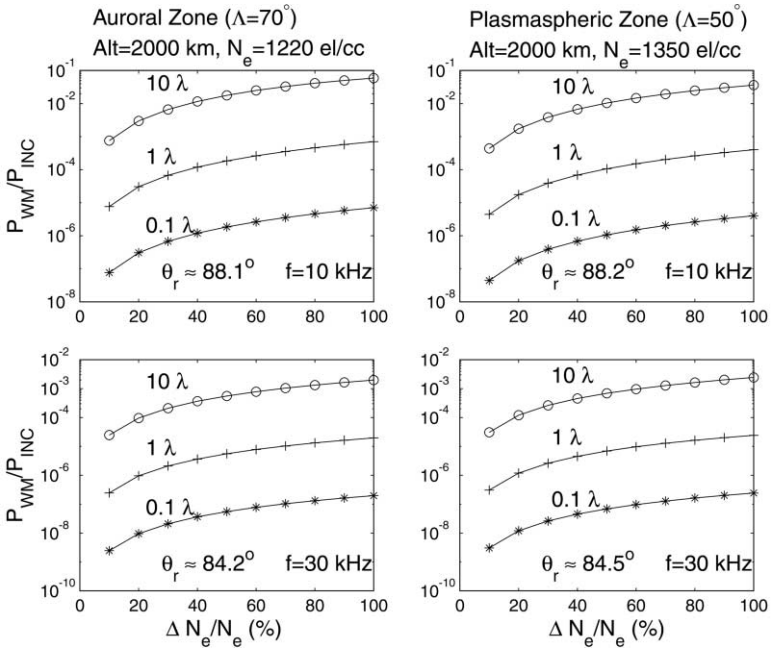

Fig. 6. The ratio of power in the small wave-normal-angle transmitted whistler-mode wave to that of the large wave-normal-angle incident wave for auroral (left panels) and plasmaspheric zones (right panels) as a function of the density enhancement within the scattering irregularity (see text for details). Cases for waves at 10 and 30 kHz are shown.

electrostatic modes with large wave vectors. Titova et al. (1984) have proposed that ion-acoustic or ion-cyclotron waves cause small-scale ionospheric irregularities that transform small-θ whistlers into large-θ whistlers by resonant scattering of VLF waves. It is possible that some of these other mechanisms may be able to convert large-θ whistler-mode waves to small-θ whistler-mode waves and could be operative alongside the passive linear scattering mode discussed in this paper.

For an RPI signal to be detectable on the ground we require that there be sufficient power in the large-wave-normal-angle wave incident at a few thousand km altitude where the meter-scale irregularities exist. It is also necessary that the incident wave-normal angle be within a degree or so of the resonance cone. Fig. 7 shows RPI signals injected parallel to the magnetic field, thus taking advantage of ~30–50 dB radiation gain. The rays reach the ionosphere in the opposite hemisphere with large-wave-normal angles, within less than a degree of the resonance cone. There is also focusing of rays in the opposite hemisphere at low altitudes. Assuming 1 W of radiated power at 10 kHz in a bandwidth of 10 Hz, 30 dB of radiation gain along the field line, and taking into account the focusing of rays, we estimate the power incident at 2000 km to be about 10^{-10} W m^{-2} Hz^{-1}, comparable to that in the auroral hiss at similar altitudes (10^{-12}–10^{-11} W m^{-2} Hz^{-1}) (Barrington et al., 1971; Gurnett and Frank, 1972). Therefore, the chances of detecting RPI signals on the ground appear to be good.

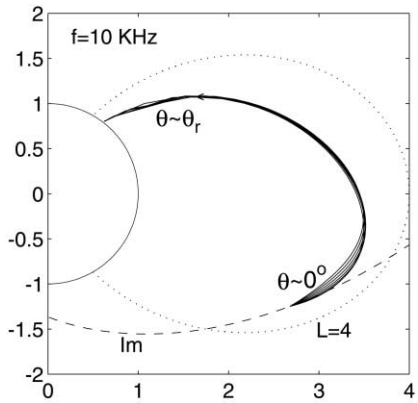

Fig. 7. Examples of nonducted ray paths from a sample IMAGE orbit that reach low altitude in the Northern hemisphere with $\theta \sim \theta_r$. These waves can penetrate to the ground by linear mode conversion. The figure also Illustrates the focusing effect at low altitudes of 10 kHz waves injected in the southern hemisphere with parallel wave-normal angle.

2.3. Wave-normal analysis of whistler-mode signals received on the IMAGE

The measurements available from the RPI receiver include the amplitude and phase of received voltages on three electric antennas. Two important propagation parameters

needed to determine the propagation path(s) of returning echoes are time delay and wave-normal direction. The time delays are easily measured from the known pulse transmission time and the time of arrival of the echo. In this section, we describe a method to measure the wave-normal direction of the returned echo. Once the time delay and the wave-normal direction are known, we can construct the propagation path of the signal with the help of ray tracing computations. Knowledge of the path will then permit diagnostic studies of the kind discussed in a later section.

2.3.1. General principles

The whistler mode wave-normal analysis method described here is based on the general formulation for satellite wave data analysis developed by Sonwalkar (1986) and Sonwalkar and Inan (1986, 1988). This formulation has been successfully used to determine the wave-normal directions of ground transmitter signals, lightning-generated whistlers, and hiss received on spacecraft equipped with various antenna configurations (single spinning electric field antenna on ISEE-1 and the Pioneer Venus Orbiter, spinning electric dipole and magnetic loop antenna on DE 1, and electric and magnetic antennas on the nonspinning COSMOS-1809 satellite) (Sonwalkar et al., 1984, 1991, 1994a; Sonwalkar and Inan, 1986, 1988; Draganov et al., 1993).

As in the more general case of waves propagating in the magnetosphere, the polarization of a whistler-mode wave ($f < f_H, f_{pe}$) for a given wave-normal direction is completely determined given the wave frequency, plasma frequencies (electron and ion densities), and gyrofrequency (magnetic field). This polarization is characterized by an electric field describing a right-hand ellipse in three dimensions. Such an ellipse is characterized by three parameters: E_0, θ, and ϕ, where E_0 is proportional to wave intensity and θ and ϕ define the direction of the wave-normal vector in a given coordinate system. Figs. 8a and b define an RPI coordinate system in which two 500-m dipole antennas are in the spin plane (xy) and the 20-m dipole is along the spin axis (z). The location of the antennas in the spin plane is characterized by a spin angle α. The angle θ_{BK} between the wave-normal vector $\mathbf{k}$ and the geomagnetic field $\mathbf{B}_0$ is generally called the wave-normal angle. For the whistler mode, the shape of the polarization ellipse is sensitive to wave-normal direction, varying from circular when the wave-normal vector is parallel to B to linear when it is close to the resonance cone angle, being elliptical for conditions in between.

The three mutually perpendicular electric field antennas available for RPI on IMAGE are sufficient to measure E_0, θ and ϕ. Physically, the polarization ellipse maps into three ellipses in three mutually perpendicular planes ($xy\ yz, zx$), and the properties of these ellipses are measured in each plane by the appropriate set of two antennas. In general, it is necessary to make both electric and magnetic field measurements to remove the ambiguity between upcoming (θ) or

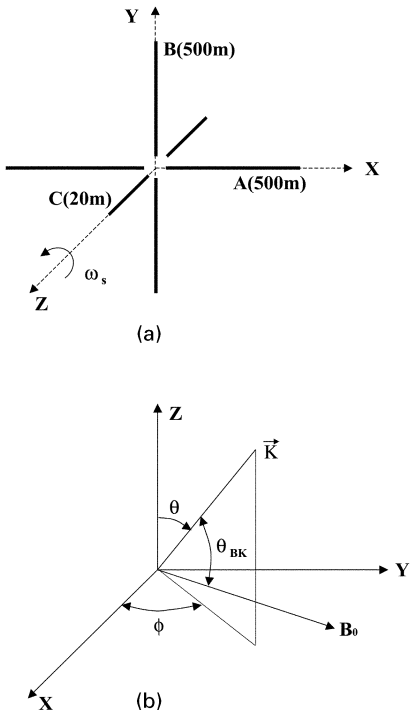

Fig. 8. (a) The geometry of antenna arrangement on the IMAGE satellite. The two 500-m long dipole antennas are in the spin plane and the 20-m dipole is along the spin axis. (b) Definitions of wave-normal angles in the antenna coordinate system.

downgoing ($180°–\theta$) waves. Nevertheless, when the wave is a coherent one of known frequency, the ambiguity can be removed in another way, even if only one type of field is being measured. The method is based on the Doppler frequency-shift due to the orbital motion of the spacecraft (Aubry, 1968). Let V_A, V_B, and V_C be the three phasors representing the magnitude and phase of the voltages across the three antennas. Then for given $\mathbf{B}_0$ and N_e, the ratios $V_B/V_A = M_{BA}\exp(j\psi_{BA})$ and $V_C/V_A = M_{CA}\exp(j\psi_{CA})$ are known functions of θ and ϕ and can be used determine the wave-normal direction. Fig. 9 schematically illustrates the wave-normal analysis method. Figs. 10a and b show the magnitudes (M_{BA}, M_{CA}) and phases (ψ_{BA}, ψ_{CA}) of the voltage ratios V_A/V_B and V_A/V_C as a function of wave-normal angle (θ_{BK}) for two values of spin angle α, assuming the wave-normal vector to be in the magnetic meridional plane (Fig. 10a) and in a plane perpendicular to that plane (Fig. 10b). In these figures it is assumed that IMAGE is located at $L = 4$ at the equator and that the local electron density is 400 el cm^{-3}.

In general, knowledge of the local plasma density and geomagnetic field is required to determine the wave-normal angle. Within the plasmasphere, whistler-mode polarization is only weakly dependent on plasma density (when the so-called QL-approximation is valid), and thus wave-normal

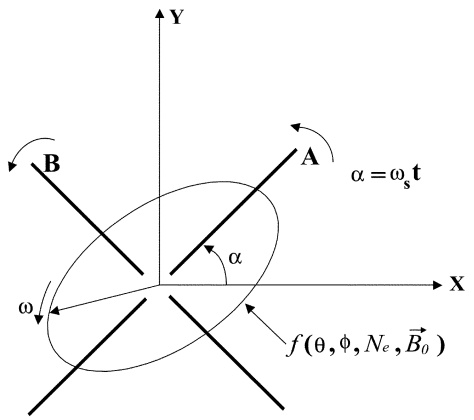

$$\frac{V_B}{V_A} = M_{\mathrm{BA}} e^{j\psi_{\mathrm{BA}}}; \qquad \frac{V_C}{V_A} = M_{\mathrm{CA}} e^{j\psi_{\mathrm{CA}}}$$

Fig. 9. A geometrical description of the wave-normal analysis method. The properties (axis ratios and orientations) of the polarization ellipses in the planes defined by the three sets of two antennas are measured by means of the phasor voltage ratios of the antenna pairs. From the measured ellipse properties the wave-normal direction is determined, assuming whistler-mode propagation. See text for details.

measurements can be made without density information. In fact, wave-normal measurements can be used to deduce the electron density by an iterative method (Sonwalkar, 1986). The electron density N_e will be measured on RPI from the local plasma resonances, and the magnitude of B_0 will be measured using an onboard magnetometer. The direction of the magnetic field can be obtained from known magnetic-field models.

2.3.2. *Wave-normal analysis of whistler-mode signals received by RPI*

One class of returning whistler-mode echoes should be in the boomerang mode, in which propagation is in the magnetic meridional plane. This simplifies wave-normal analysis, since it is not necessary to measure the azimuthal angle. Furthermore, if the hemisphere of reflection is known (from the magnitude of time delay), the θ or $(180^\circ - \theta)$ ambiguity is removed and phase measurements are not required (although these will be available). Thus, two 500-m dipoles are sufficient for measurement of the wave-normal angle of the RPI echo in the boomerang mode. For echoes returning off the meridian plane, three antennas are needed to measure the wave normal direction. The 20-m dipole perpendicular to the spin plane may cause noise problems due to the local electrostatic wave and hiss background. This problem can probably be overcome using digital signal processing techniques and noting that the echo will be a narrowband coherent signal and that the background noise will be broadband and incoherent.

2.3.3. *Analysis of multiple returning echoes*

When a transmitted signal reflects at ionospheric heights, gradients of plasma density may be present which can lead to multipath propagation and thus multiple echoes arriving at the satellite (Sonwalkar et al., 1984). The multipath signals can lead to fading of signals at differential doppler shift frequencies of the order of 1 Hz. To resolve these multiple paths there is a need for pulse duration longer than 1 s, in conflict with the usual requirement for pulses of <1 s in duration (so as to avoid overlap of the transmitted and echo signals). However, if a single wave-normal analysis is performed on the multiple echoes in a returning signal, an average wave-normal angle for the signal may be obtained (the individual wave-normal angles weighted by their respective strengths) (Sonwalkar, 1986; Sonwalkar and Inan, 1988).

2.3.4. *Wave-normal analysis of ground transmitter signals and natural signals*

When RPI is operating in the passive mode, the wave-normal analysis method described above can also be used to determine the wave-normal directions of ground transmitter signals and naturally occurring plasma waves. RPI, by providing a transmitter/receiver pair on a satellite to complement ground transmitter/receiver pairs, offers a unique basis for carrying out satellite-ground experiments to test the reciprocity of satellite-ground propagation links at VLF (see discussion in Section 2.2.3).

2.4. *Wave-particle interactions induced by RPI transmissions*

Experience with ground-based wave injection experiments suggests that transmissions from a transmitter in situ such as that of RPI can under appropriate circumstances couple strongly to the hot plasma, giving rise to wave growth of several tens of dB and to significant perturbations in the hot electron distribution function. Fig. 11, from Sonwalkar et al. (1997), shows some of the nonlinear effects that have been observed at a ground receiver near $L = 4.5$ in Canada following injection of weak coherent signals into magnetospheric paths in the outer plasmasphere from Siple, Antarctica. Fig. 11a is a spectrogram of two signals, one a falling frequency ramp and the other a constant frequency 2-s pulse. Fig. 11b shows the amplitude during the second pulse within a 100 Hz band centered on the pulse frequency. The effects of what has been called the CWI, or coherent wave instability, are indicated, including exponential wave growth by $\sim$30 dB, saturation, development of sidebands, and triggering of an emission (e.g. Helliwell, 1988). The coherence of the injected signal was found to be a key factor in these experiments (Helliwell, 1988); an amplitude threshold for wave growth was also found (Helliwell

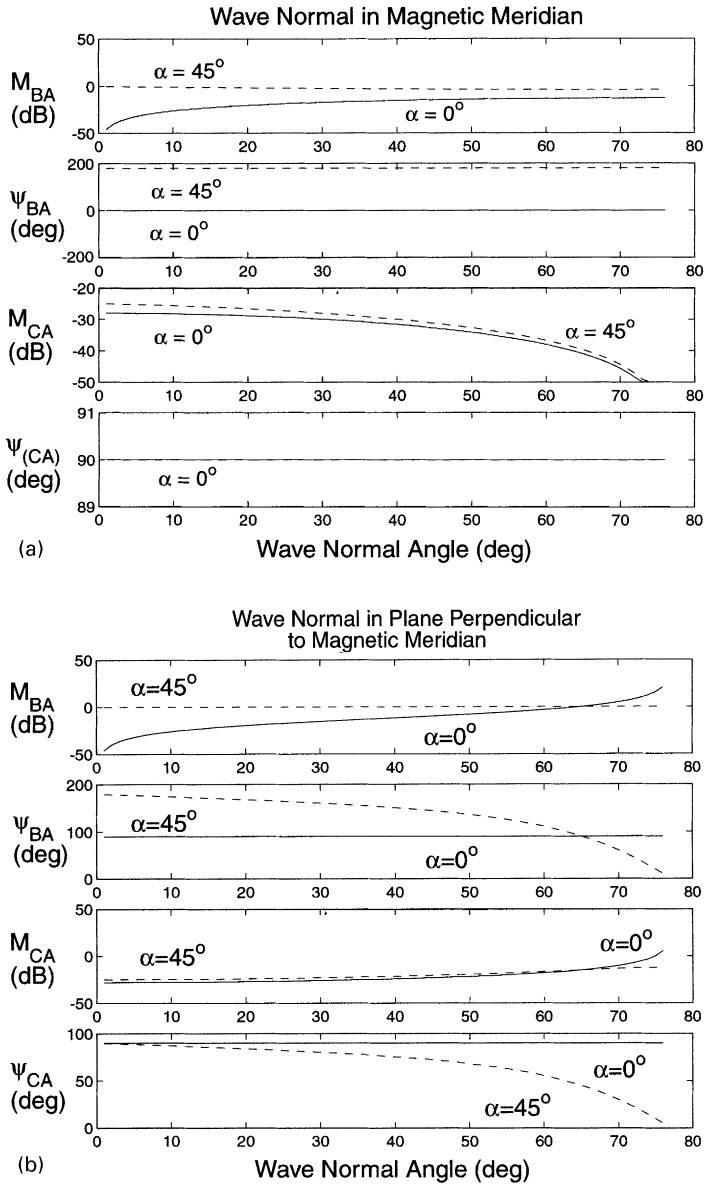

Fig. 10. The magnitude and phase of the voltage ratios as a function of wave-normal angle for (a) wave-normal vector in the magnetic meridional plane, and (b) wave-normal vector in a plane perpendicular to the magnetic meridional plane. The IMAGE satellite is assumed to be located at $L = 4$ with local electron density 400 el cm^{-3}.

et al., 1980; Mielke, 1992), but in many cases was exceeded by the weak injected signals. In one case, signals from Siple showing evidence of wave growth continued to be observed at the conjugate station as the transmitter power was stepped down from ~100 kW (~1 kW radiated) to 1 kW (~10 W radiated) (Helliwell et al., 1980).

Ground-based experiments have also provided indications of changes in the phase-space density of particles in resonance with, or nearly in resonance with, injected waves that have experienced wave growth of the type illustrated in Fig. 11. One such indication is the suppression of existing incoherent noise in a narrow band ~100 Hz below the frequency of a transmitted signal (Raghuram et al., 1977). Another, much rarer, event is the temporary reduction in the total growth of transmitted signals following the first of a series of identical pulses (Sonwalkar et al., 1995).

In an earlier section on antenna impedance and efficiency, we concluded that the wave power within 100 km of the RPI transmitter should be greater than that produced by wave injection from Siple, Antarctica. We thus conclude

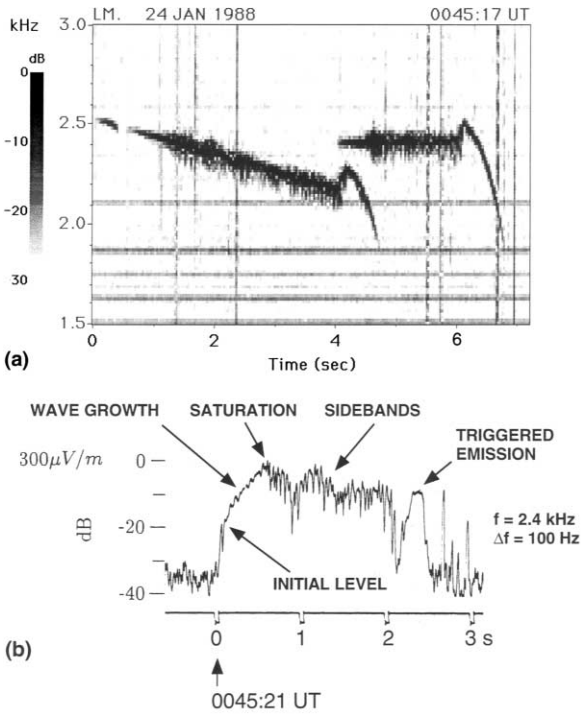

Fig. 11. (a) Spectrogram of Siple transmitter signals, the slow ramp and 2-s constant power and constant-frequency pulse, as they were received at Lake Mistissini at ~0045 UT on January 24, 1988. (b) Chart showing amplitude variations within a 100-Hz band centered on frequency of the constant-frequency pulse and beginning just prior to the start of the pulse. The zero of the timescale of the spectrogram represents the leading edge of the 2-s pulse as it was radiated at Siple station, while the zero below the amplitude record refers to $t = 4$ s on the spectrogram scale, or the approximate arrival of the leading edge of the 2-s pulse at the receiver (from Sonwalkar et al., 1997).

that whistler-mode signals from RPI can couple strongly to the hot plasma and give rise to effects similar to those illustrated in Fig. 11. Given that substantial wave growth of the transmitter signals can occur, we would also expect RPI to induce noise suppression effects of the kind noted above.

Key issues now concern the circumstances under which wave–particle interactions can be induced and the extent to which the interactions can be detected on IMAGE, on other satellites, and on the ground. The strongest wave–particle interactions would appear possible when the satellite is in the outer plasmasphere and in the vicinity of the equator, so as to take advantage of the extended near-equatorial regions where the conditions for resonance with waves of a given frequency change only slowly with distance along a geomagnetic field line. If wave–particle interactions involving RPI pulses then occur, but in the absence of significant field-aligned irregularities, the resulting waves would not be expected to echo back to the satellite because of the ray bending mentioned above. However, if another satellite such as Akebono is in rendezvous, as discussed earlier, there is a good chance that it will detect the signal, particularly after the signal has undergone ionospheric reflection at low altitude.

If waves near $f_H/2$ are launched at small wave-normal angles and a guiding structure or duct is excited, the associated plasma density gradients may restrict the wave-normals to a narrow range around the field direction. Propagation will then continue down into the ionosphere, where the waves may exit the duct or guiding structure. Some fraction of the wave energy may then penetrate the ionosphere and be detected at ground stations, while the remaining energy should be reflected upward as the sharp gradients in refractive index at the lower edge of the ionosphere are encountered. After reflection the waves may then propagate in essentially a non-ducted manner to the satellite or to other satellites at nearby longitudes. This hybrid mode, by which waves that are initially guided spread so as to reach much larger field-line regions, has been frequently identified through passive satellite wave experiments (Rastani et al., 1985; Bell et al., 2000). There is also the possibility of reexcitation of the original guiding path after reflection, followed by return propagation in the ducted mode to the satellite.

3. Main science questions to be addressed

3.1. Introduction

The problem areas to be addressed through whistler-mode probing include: (1) the physics of wave–particle energy and momentum exchange within and near the plasmasphere; (2) the behavior of electric antennas at whistler-mode frequencies during in situ wave injection experiments; (3) plasmaspheric density structure and its influence on whistler-mode propagation; (4) the downward penetration of the ionosphere by whistler-mode signals. The problem of the behavior of electric antennas at whistler-mode frequencies under conditions of high applied voltage was introduced in an earlier section, as was the question of downward penetration of the ionosphere. Below, we briefly discuss the other two topics, noting that some of the outstanding problems in hot plasma diagnostics have been discussed by Helliwell (1988), and that problems in plasmasphere structure have been discussed in a recent paper by Carpenter and Lemaire (1997).

3.2. Hot plasma diagnostics; excitation of VLF emissions

Whistler-mode waves are believed to play a critical role in the redistribution and loss of radiation belt particles, but the details of the origin of the waves and of their resonance interactions with the particles are not yet well known and in some cases are controversial. Observations suggest that geophysically important interactions may occur in the case of both hiss-like, incoherent wave activity as well as narrow-band, quasi-coherent waves.

(a) What is the nature of the so-called "interaction region", in which temporal growth of coherent waves appears to occur? It has been suggested that temporal growth of a quasi-coherent signal in the magnetosphere is concentrated within a limited region along the signal path where the spatial variation in the conditions for cyclotron resonance as seen by the particles is minimal, as in the equatorial region in the case of constant frequency waves, or where that variation is closely matched to the frequency variations in the input wave, as in off-equatorial regions (e.g. Helliwell, 1967, 1970). However, recent observations (Bell et al., 2000) suggest that the interaction region is defined by the spatial distribution of the energetic electron population. Within an interaction region, cyclotron resonance between waves and particles can be sustained long enough to achieve a significant exchange of energy and momentum, and temporal growth can occur through a feedback process (e.g. Helliwell and Inan, 1982). Ground-based wave injection experiments have told us much about the output from active signal paths under various conditions on the waveform of the input. However, RPI experiments would provide previously unavailable opportunities to probe the interaction region from a wide variety of locations in space and very likely from within or very near the region itself. Thus, one could further test the concept of the interaction region and investigate important questions that have been raised in the literature about the input intensity of a coherent wave required to initiate temporal wave growth (e.g. Helliwell and Walworth, 1996).

(b) What effect does the coherent wave instability have on the phase-space distribution of resonant particles? RPI can provide new insight into wave-induced phase-space perturbations by detecting the suppression of incoherent whistler-mode noise associated with injected coherent waves. The RPI receiver with $\sim$300 Hz bandwidth can be used to monitor changes in background noise near a transmitter frequency whether or not whistler-mode echoes of those transmissions are received on the satellite. The expected ability to launch signals at higher input levels than those achieved in the Siple ground experiments increases the probability of detecting temporary reductions in wave growth at the transmitter frequency itself.

(c) What controls the input wave threshold intensity level above which temporal growth can occur? It has been proposed that the threshold is controlled by the level of incoherent in situ noise at the relevant frequencies (e.g. Mielke and Helliwell, 1992). RPI can provide new insight into the growth threshold question by acquiring information on the relationship between in situ noise level and perturbations in the noise spectrum indicative of wave growth.

3.3. Whistler-mode probing of plasmasphere density structure

There are important unanswered questions about the density structure of the plasmasphere. The manner in which its internal structure changes during a cycle of plasmasphere-erosion and recovery is poorly known (e.g. Carpenter, 1995). Irregular structure has been found to appear both in the outer part of a recently eroded plasmasphere and in the plasmapause region itself, but the origin of the irregularities and their geophysical importance are not well understood (e.g. Carpenter and Lemaire, 1997). Density cavities in the plasmasphere occur through processes yet to be established (Carpenter et al., 2000). The distribution of plasma along the field lines within the eroded plasmasphere or in the recovering plasma trough beyond is not well known, especially during periods of recovery from disturbance. The distribution transverse to **B** of plasma density structures (ducts) that guide whistler-mode waves between conjugate ground points is not well known, and the origin of the structures is not understood.

New knowledge of plasmasphere density structure derived from IMAGE will shed light on the manner in which whistler-mode waves propagate so as to literally fill large regions of the magnetosphere. This question arises because of the important role that waves play in moderating the levels of energetic particles in the Earth's radiation belts. The issue is complicated by the fact that waves involved in a particular interaction do not necessarily originate at the time of the interaction or on the field lines involved. The complexities of propagation are not easy to investigate from passive satellite experiments that detect ground- and space-originated whistler-mode signals but do not obtain data on density structure affecting the paths of those signals.

3.3.1. Density cavities in the plasmasphere

Whistler-mode signals from RPI can probe several important forms of field-aligned structure. One is the "inner trough", which typically involves density depressions by factors of from 3 to 5 within the plasmasphere [Carpenter et al., 2000]. These depressions have been found to extend inward to $L<2.5$ and to occur in field-aligned regions that may be extensive in longitude, as evidenced by the fact that they can trap continuum radiation extending well above the escape frequency for such radiation from the outer magnetosphere. Their origin has yet to be determined, but they are believed to develop as a consequence of the plasmasphere erosion process associated with periods of enhanced convection.

Such density cavities, ranging in width from $\Delta L\sim0.5$ to 1.5, may be difficult to detect from high-altitude photon images or from RPI sounding. However, as RPI penetrates a cavity, the group delays of any received ducted and non-ducted whistler-mode signals will register the low-density levels and also reveal the presence of cavity boundaries through evidence of gradient trapping of the waves. The outer boundaries of the cavities are often very abrupt, with electron density changing by a factor of $\sim$5 within <100 km near the equator.

3.3.2. Density irregularities in the plasmapause region

Density irregularities with high peak to valley ratios, in the range ~2–5 occur regularly near the plasmapause in the aftermath of disturbance (e.g. Koons, 1989; LeDocq et al., 1994; Moldwin et al., 1995; Carpenter, 1997). Scale lengths vary from less than a few hundreds km to several thousands km. The mechanisms that give rise to these structures are not known, although a variety of instabilities have been proposed (e.g. Kelley, 1989; Lemaire, 1987). When passing through such regions, as opposed to probing them from outside, much can be learned by operating the satellite receiver in the whistler-mode range, as well as by relaxation sounding for density information. The irregularities should in some cases efficiently trap and guide whistler-mode magnetospheric noise, including any signals that can be transmitted by RPI.

3.3.3. Field-aligned wave ducts

In the real plasmasphere, a small but poorly known fraction of the volume is occupied by field-aligned density structures (ducts) or irregularities (such as the plasmapause) that constrain the wave-normals and cause the waves to be guided along the field lines. Excitation of guided paths by RPI would be expected to occur either due to trapping along "one-sided" ducts, where there is a region of steep negative gradient in the density, or because of transmitting within, or leaking into, quasi-cylindrical ducts of locally enhanced electron density.

The reception of ducted echoes will provide a unique way of identifying and studying the occurrence of whistler ducts. The physical basis for the occurrence of ducts remains to be understood. Until now direct detection of ducts or of propagation therein has been quite limited, partly because of the relatively small volume of the magnetosphere that ducts may occupy, and partly because of the density enhancement factors in quasi-cylindrical ducts are believed to be small, in the 10% range (e.g. Smith and Angerami, 1968; Angerami, 1970; Scarf and Chappell, 1973; Carpenter et al., 1981; Koons, 1989).

3.3.4. The poorly known density distribution along geomagnetic field lines

In the "boomerang" mode, waves return to the satellite following reflection at the LHR. For a given transmitted frequency above the local LHR frequency, the point of reflection at a lower altitude (where the pulse and LHR frequencies become equal) can be estimated from a magnetic field model, since the LHR at any point is approximately equal to $f_H/43$, where f_H is the local electron gyrofrequency. The observed echo delay may then be used to provide an integral measure of the plasma density along the magnetic field to the reflection point. As transmitter frequency is then increased, the echo delay will tend to increase due to the growing distance to the corresponding LHR reflection point (the analysis is simplified by the fact that for wave-normals at the so-called Gendrin angle (Gendrin, 1961), for which the ray direction is along the magnetic field, the group velocity is independent of frequency). A combination of data on local density at the satellite and multifrequency boomerang mode delays may then make possible a multiparameter analysis of the density distribution along the field-line. (The range of frequencies within which the boomerang mode might be observed from a given satellite location remains to be estimated.)

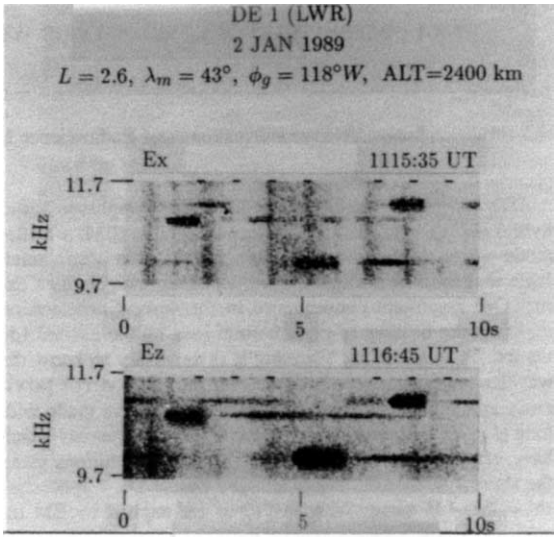

Fig. 12. DE 1 observations of lower hybrid waves excited by signals from the Omega (ND) transmitter. The top and bottom panels, respectively, show reception by E_x and E_z antennas. The E_x antenna consists of two 100 m wires deployed in the spin plane. The E_z antenna consists of two 4 m tubes deployed along the spin axis (from Bell et al., 1991).

If guided or ducted echoes are received, their group delays can be used to measure the integrated plasma density from the spacecraft to the lower ionosphere boundary in one or both directions along the field lines, as in the case of the boomerang mode. This information, combined with local measurements of density from relaxation sounding over the full RPI range or from conventional sounding from exterior locations, can provide new information on the distribution of plasma along the magnetic field, as well as much improved empirical data on the overall plasmasphere density distribution.

3.3.5. Lower hybrid wave excitation and probing of irregular density structure

In previous satellite experiments, it has been found that whistler-mode wave energy in the magnetosphere is regularly transformed into quasi-electrostatic waves at frequencies just above the lower hybrid resonance frequency (LHR) (Bell and Ngo, 1988, 1990). A particularly well-defined example of this effect occurs in the lower ionosphere, when strong signals from ground VLF transmitters encounter

small-scale irregularities. Fig. 12 shows DE 1 observations of quasi-electrostatic whistler mode waves (lower hybrid waves) excited by signals from the Omega (ND) transmitter. At an irregularity boundary a portion of the incident wave is coupled into quasi-electrostatic modes. The wave length of these modes is determined by the spatial scales of the irregularities. On moving spacecraft the doppler shifts of the quasi-electrostatic modes can be measured and their wavelengths determined. This determination then provides information on the spatial scales of the irregularities and the poorly known power spectral density of irregularities of scale size 1–100 m. The idea for RPI would be to launch whistler-mode waves just above the LHR, say by operations in the ~10–12 kHz range (this is a modification of the strategy for achieving ionospheric penetration discussed earlier). Reflections would occur near 500–600 km altitude, and the occurrence of mode conversion would be indicated by the presence of doppler shifted quasi-electrostatic modes propagating up to the spacecraft from the irregular region below.

4. Concluding remarks

This paper discusses the feasibility of conducting whistler-mode wave-injection experiments within and near the plasmasphere and the potential of such experiments to address certain science questions. We have considered various feasibility issues within the general context of space-based VLF wave experiments as well as in the specific case of the RPI instrument on the IMAGE satellite. We find that there is a good chance that RPI signals will be detectable: (1) on IMAGE as returning echoes; (2) on a satellite of opportunity such as Akebono; (3) on the ground. Outstanding science problems that can be addressed through VLF wave-injection experiments from space involve: (1) properties of a VLF antenna operating at high voltages in space, (2) energy and momentum exchange during wave–particle interactions in the outer plasmasphere, (3) identification of cold-plasma density structures and boundaries of various scale sizes and their effects on wave propagation; and (4) factors governing penetration of VLF signals to the ground. We believe that whistler-mode wave injection experiments from space can provide substantial new understanding of the inner magnetosphere.

Acknowledgements

We thank R.A. Helliwell and L.R.O. Storey for many useful comments. This research was supported by the Los Alamos National Laboratory under contract 389AZ0017-97 to the University of Alaska Fairbanks.

References

Angerami, J.J., 1966. A whistler study of the distribution of thermal electrons in the magnetosphere. Ph.D. Dissertation, Radioscience Laboratory, Stanford University.

Angerami, J.J., 1970. Whistler duct properties deduced from VLF observations made with the OGO-3 satellite near the magnetic equator. Journal of Geophysical Research 75 (31), 6115.

Angerami, J.J., Thomas, J.O., 1964. Studies of planetary atmosphere 1, the distribution of electrons and ions in the Earth's exosphere. Journal of Geophysical Research 69, 4537.

Aubry, M.P., 1968. Some results of the FR-1 satellite experiment in the zone close to the transmitter. Journal of Atmospheric and Terresterial Physics 30, 1161–1182.

Barrington, R.E., Hartz, T.R., Harvey, R.W., 1971. Diurnal distribution of ELF, VLF and LF noise at high latitudes as observed by Alouette — 2. Journal of Geophysical Research 76, 5278.

Bell, T.F., Inan, U.S., Helliwell, R.A., Scudder, J.D., 2000. Simultaneous triggered VLF emissions and energetic electron distributions observed on POLAR with PWI and HYDRA. Geophysical Research Letters 27, 165–168.

Bell, T.F., Ngo, H.D., 1988. Electrostatic waves stimulated by coherent VLF signals propagating in and near the inner radiation belt. Journal of Geophysical Research 93, 2599.

Bell, T.F., Ngo, H.D., 1990. Electrostatic lower hybrid waves excited by electromagnetic whistler mode waves scattering from planar magnetic-field-aligned plasma density irregularities. Journal of Geophysical Research 95, 149.

Burgess, W.C., Inan, U.S., 1993. The role of ducted whistlers in the precipitation loss and equilibrium flux of radiation belt electrons. Journal of Geophysical Research 98 (A9), 15,643.

Carpenter, D.L., 1966. Whistler studies of the plasmapause in the magnetosphere, 1: Temporal variations in the position of the knee and some evidence on plasma motions near the knee. Journal of Geophysical Research 71, 693.

Carpenter, D.L., 1995. Earth's plasmasphere awaits rediscovery. EOS 76, 89–92.

Carpenter, D.L., 1997. Lightning whistlers reveal the plasmapause, an unexpected boundary in space, discovery of the magnetosphere. History of Geophysics 7, 47.

Carpenter, D.L., Anderson, R.R., Bell, T.F., Miller, T.R., 1981. A comparison of equatorial electron densities measured by whistlers and by a satellite radio technique. Geophysical Research Letters 8 (10), 1107.

Carpenter, D.L., Anderson, R.R., Calvert, W., Moldwin, M.B., 2000. CRESS observations of density cavities inside the plasmasphere. Journal of Geophysical Research 105 (A10), 23,323.

Carpenter, D.L., Bao, Z.T., 1983. Occurrence properties of ducted, whistler-mode signals from the new VLF transmitter at Siple Station, Antarctica. Journal of Geophysical Research 88, 7051.

Carpenter, D.L., Lemaire, J., 1997. Erosion and recovery of the plasmasphere in the plasmapause region. Space Science Reviews 80, 153.

Carpenter, D.L., Miller, T.R., 1976. Ducted magnetospheric propagation of signals from the Siple, Antarctica, VLF transmitter. Journal of Geophysical Research 81, 2692.

Draganov, A.B., Inan, U.S., Sonwalkar, V.S., Bell, T.F., 1993. Whistlers and plasmaspheric hiss: wave directions and three-dimensional propagation. Journal of Geophysical Research 98, 11,401–11,410.

Edgar, B.C., 1972. The structure of the magnetosphere as deduced from magnetospherically reflected whistlers. Ph.D. Thesis, Stanford University.

Eviatar, A., Lenchek, A.M., Singer, S.F., 1964. Distribution of density in a ion-exosphere of a nonrotating planet. Physics of Fluids 7, 1775–1779.

Gendrin, R., 1961. Le guidage des whistlers par le champ magnetique. Planetary Space Science 5 (4), 274.

Groves, K.M., Lee, M.C., Kuo, S.P., 1988. Spectral broadening of VLF radio signals traversing the ionosphere. Journal of Geophysical Research 93, 14,683.

Gurnett, D.A., Frank, L.A., 1972. VLF hiss and related plasma observations in the polar magnetosphere. Journal of Geophysical Research 77, 172.

Gurnett, D.A., Inan, U.S., 1988. Plasma wave observations with the Dynamics Explorer 1 spacecraft. Reviews of Geophysics 26, 285.

Helliwell, R.A., 1965. Whistlers and Related Ionospheric Phenomena. Stanford University Press, Stanford, California.

Helliwell, R.A., 1967. A theory of discrete VLF emissions from the magnentosphere. Journal of Geophysical Research 72, 4773.

Helliwell, R.A., 1970. Intensity of discrete VLF emissions. In: McCormac, B.M. (Ed.), Particles and Fields in the Magnetosphere, D. Reidel, Dordrecht, Amsterdam, p. 292.

Helliwell, R.A., 1988. VLF wave stimulation experiments in the magnetosphere from Siple Station, Antarctica. Reviews of Geophysics 26, 551.

Helliwell, R.A., 1995. The role of the Gendrin mode of VLF propagation in the generation of magnetospheric emissions. Geophysical Research Letters 16, 2095–2098.

Helliwell, R.A., Carpenter, D.L., Miller, T.R., 1980. Power threshold for growth of coherent VLF signals in the magnetosphere. Journal of Geophysical Research 85, 3360.

Helliwell, R.A., Inan, U.S., 1982. VLF wave growth and discrete emission triggering in the magnetosphere: a feedback model. Journal of Geophysical Research 87, 3537.

Helliwell, R.A., Katsufrakis, J.P., 1974. VLF wave injection into the magnetosphere from Siple Station, Antarctica. Journal of Geophysical Research 79, 2511.

Helliwell, R.A., Walworth, K.F., 1996. Whistler mode wave intensities in the radiation belts. In: Reeves, G.D. (Ed.), Workshop on the Earth's Trapped Particle Environment. AIP Press, Woodbury, NY, pp. 61–63.

Inan, U.S., Bell, T.F., 1977. The plasmapause as a VLF wave guide. Journal of Geophysical Research 82 (19), 2819.

Inan, U.S., Bell, T.F., Helliwell, R.A., Katsufrakis, J.P., 1981. A VLF transmitter on the Space Shuttle. Advances in Space Research 1, 235.

James, H.G., 1972. Refraction of whistler-mode waves by large-scale gradients in the middle latitude ionosphere. Annals of Geophysics 28, 301.

Kelley, M., 1989. The Earth's Ionosphere. Academic, San Diego, CA.

Kimura, I., 1966. Effects of ions on whistler-mode raytracing. Radio Science 1, 269.

Kintner, P.M., Brittain, R., Kelley, M.C., Carpenter, D.L., Rycroft, M.J., 1983. In situ measurements of transionospheric VLF wave injection. Journal of Geophysical Research 88, 7065–7073.

Koons, H.C., 1989. Observations of large-amplitude, whistler mode wave ducts in the outer plasmasphere. Journal of Geophysical Research 94, 15,393.

LeDocq, M.J., Gurnett, D.A., Anderson, R.R., 1994. Electron number density fluctuations near the plasmapause observed by the CRRES spacecraft. Journal of Geophysical Research 99, 23,661.

Lemaire, J., 1987. The plasmapause formation. Physica Scripta T18, 111–118.

Mielke, T.A., Helliwell, R.A., 1992. An experiment on the threshold effect in the coherent wave instability. Geophysical Research Letters 19, 2067.

Mlodnosky, R.F., Garriott, O.K., 1963. Proceedings of International Conference on the Ionosphere, The Institute of Physics and the Physical Society, 484.

Moldwin, M.B., Thomsen, M.F., Bame, S.J., McComas, D.J., Reeves, G.D., 1995. The fine scale structure of the outer plasmasphere. Journal of Geophysical Research 100, 8021.

Ngo, Hoc D., 1989. Electrostatic waves stimulated by VLF Whistler mode waves scattering from magnetic-field-aligned plasma density irregularities, Ph.D. Thesis, Stanford University.

Park, C.G., 1982. Whistlers. In: Volland, V. (Ed.), Handbook of Atmospherics, Vol. 2. CRC Press, Boca Raton, FL, pp. 21–77.

Persoon, A.M., 1988. Electron density distributions in the high-latitude magnetosphere. Advances in Space Research 8 (8), 79–88.

Raghuram, R., Bell, T.F., Helliwell, R.A., Katsufrakis, J.P., 1977. Quiet band produced by VLF transmitter signals in the magnetosphere. Geophysical Research Letters 4 (5), 199.

Rastani, K., Inan, U.S., Helliwell, R.A., 1985. DE-1 observations of Siple transmitter signals and associated sidebands. Journal of Geophysical Research 90, 4128.

Reinisch, B.W., Haines, D.M., Bibl, K., Cheney, G., Galkin, I.A., Huang, X., Myers, S.H., Sales, G.S., Benson, R.F., Fung, S.F., Green, J.L., Taylor, W.W.L., Bougeret, J.-L., Manning, R., Meyer-Vernet, N., Moncuquet, M., Carpenter, D.L., Gallagher, D.L., Reiff, P., 2000. The radio plasma imager investigation on the IMAGE spacecraft. Space Science Reviews, IMAGE Special Issue 91, 319.

Sawada, A., Nobata, T., Kishi, Y., Kimura, I., Oya, H., 1993. Electron density profile in the magnetosphere deduced from in situ electron density and wave normal directions of Omega signals observed by the Akebono (EXOS D) satellite. Journal of Geophysical Research 98, 11,267.

Scarf, F.L., Chappell, C.R., 1973. An association of magnetospheric whistler dispersion characteristics with changes in local plasma density. Journal of Geophysical Research 78, 1597.

Smith, R.L., Angerami, J.J., 1968. Magnetospheric properties deduced from OGO 1 observations of ducted and non-ducted whistlers. Journal of Geophysical Research 73 (1), 1.

Sonwalkar, V.S., 1986. New signal analysis techniques and their applications to space physics. Ph.D. Thesis, Stanford University.

Sonwalkar, V.S., 1995. Magnetospheric LF-, VLF-, and ELF-waves. In: Volland, H. (Ed.), Handbook of Atmospheric Electrodynamics, CRC Press, Boca Raton, FL, Vol. II (Chapter 13).

Sonwalkar, V.S., Harikumar, J., 2000. An explanation of ground obesrvations of auroral hiss: role of density depletions and meter-scale irregularities. Journal of Geophysical Research 105 (A8), 18,867.

Sonwalkar, V.S., Bell, T.F., Helliwell, R.A., Inan, U.S., 1984. Direct multiple path propagation: a fundamental property of nonducted VLF waves in the magnetosphere. Journal of Geophysical Research 89, 2823–2830.

Sonwalkar, V.S., Carpenter, D.L., Helliwell, R.A., Walt, M., Inan, U.S., Caudle, D.L., Ikeda, M., 1997. Properties of the magnetospheric hot plasma distribution deduced from whistler mode wave injection at 2400 Hz: ground-based detection of

azimuthal structure in magnetospheric hot plasmas. Journal of Geophysical Research 102, 14,363–14,380.

Sonwalkar, V.S., Carpenter, D.L., Strangeway, R.J., 1991. Testing radio bursts observed on the nightside of Venus for evidence of whistler mode propagation from lightning. Journal of Geophysical Research 96, 17,763–17,778.

Sonwalkar, V.S., Chang, L., Walworth, K., Carpenter, D.L., Helliwell, R.A., Walt, M., Inan, U.S., 1995. Siple station wave injection experiments: 'first pulse suppression' of emission activity. EOS Transactions 76, 46.

Sonwalkar, V.S., Inan, U.S., 1986. Measurement of Siple transmitter signal on the DE–1 satellite: wave-normal direction and antenna effective length. Journal of Geophysical Research 91, 154–164.

Sonwalkar, V.S., Inan, U.S., 1988. Wave-normal direction and spectral properties of whistler-mode hiss observed on the DE-1 satellite. Journal of Geophysical Research 93, 7493–7514.

Sonwalkar, V.S., Inan, U.S., Bell, T.F., Helliwell, R.A., Chmyrev, V.M., Sobolev, Ya.P., Ovcharenko, O.Ya., Selegej, V., 1994a. Simultaneous observations of VLF ground transmitter signals on the DE 1 and COSMOS 1809 satellites: detection of a magnetospheric caustic and a duct. Journal of Geophysical Research 99, 17,511–17,522.

Sonwalkar, V.S., Inan, U.S., Bell, T.F., Helliwell, R.A., Molchanov, O.A., Green, J.L., 1994b. DE 1 VLF observations during Activny wave injection experiments. Journal of Geophysical Research 99, 6173.

Titova, E.E., Di, V.I., Yurov, V.E., Raspopov, O.M., Trakhtengertz, V.Yu., Jiricek, F., Triska, P., 1984. Interaction between VLF waves and turbulent ionosphere. Geophysical Research Letters 11, 323.

Tsuruda, K., Machida, S., Terasawa, T., Nishida, A., Maezawa, K., 1982. High spatial attenuation of the Siple transmitter signal and natural VLF chorus observed at ground-based chain stations near Roberval, Quebec. Journal of Geophysical Research 87, 742.

Tsuruda, K., Oya, H., 1993. Introduction to the Akebono (EXOS D) project. Journal of Geophysical Research 98, 11,123.

Wang, T.N.C., 1970. Tech. Rep. 3414-1, Radioscience Lab. Stanford Electron. Lab., Stanford University, Stanford, Calif. 94,305.

Wang, T.N.C., Bell, T.F., 1972. VLF/ELF radiation patterns of arbitrarily oriented electric and magnetic dipoles in a cold lossless multicomponent magnetoplasma. Journal of Geophysical Research 77, 1174.